

NONLINEAR FINITE ELEMENT ANALYSIS OF PRESTRESSED CONCRETE MEMBERS

Dr. Hani M. Fahmi,
Professor in Civil Engineering Department,
Nahrain University.
e-mail: fahmihanim@yahoo.com

Dr. Zubaidah A. Al-Bayati
Lecturer in Civil Engineering Department,
Al-Mustansiriya University.
e-mail: zubaidah_albayati@yahoo.com

Abstract

A finite element method of analysis is used to study the strength and behavior of prestressed concrete members under short-term and sustained load conditions. The degenerated assumed strain eight-node shell finite element is used with each node having five degrees of freedom. Material nonlinearity has been included in the analysis. Concrete is considered as an elastic-plastic material in compression with strain hardening, prestressing tendons are modeled by a multi-linear five branches stress-strain relationship. The layered approach is used to represent the concrete whereas the prestressing tendons are modeled as axial members embedded within the concrete elements.

A computer program is developed and used for the analysis of prestressed concrete members having arbitrary tendon layout in either pretensioned or post-tensioned tendons. The tendon layout is specified and the loading due to prestressing is numerically calculated using the computer program. The validity of the proposed model for embedded bar representation of the prestressing tendons and the developed method of prestressing force inclusion into the entire member is demonstrated. The capabilities of the computer program resulting from the present developments are verified by analyzing experimentally tested prestressed concrete slabs. The computed results are compared with the available experimental data. The comparison verified the accuracy and adequacy of the method and models used utilizing the developed computer program.

1. Introduction

Prestressed concrete construction is an alternative technique to that of conventional reinforced concrete. In the early days of reinforced concrete construction, the available steel did not have sufficient strength for prestressing work, but the development of high-strength reinforcement soon led to a more widespread acceptance of this construction material. The availability of high

strength steel was also matched by improvements in concrete technology, resulting in the availability of high strength of concrete, which is more suitable for prestressing work.

To assess the factor of safety against collapse and satisfy the continuous demand for longer spans and thinner members, the ultimate load capacity and the serviceability of the structure throughout its useful life have to be ensured. In this case, a linear analysis may not be sufficient [1].

In the present research work develops a method for the formulation of prestressing force and its effects on the strength and behavior of prestressed concrete members with the aid of nonlinear finite element analysis using the degenerated shell element utilizing a specially prepared computer program.

2. Theoretical Approach

The degenerated shell element procedure which was originally introduced by Ahmad et al. [2], and shown in Figs.1 and 2, is used in the current research work. If the shell is built up from a series of layers of different materials, such that the material properties (and stress) are discontinuous

functions of ζ , an appropriate integration through the thickness has to be carried out. These factors are accommodated in a simple and effective manner by using a layered approach, where a mid-point integration scheme is adopted for each layer.

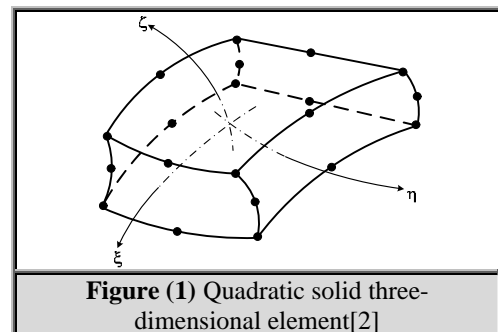


Figure (1) Quadratic solid three-dimensional element[2]

In the nonlinear finite element analysis of reinforced thin plate structures, the steel reinforcement is usually represented as a smeared layer. Alternatively, when there is a lumped area of steel at a certain location, like the main steel bars in beams or prestressing tendons, the reinforcement is usually represented as a single discrete bar element connected to the nodes of adjacent concrete elements.

When shell elements are used to model reinforced concrete structures, the discrete bar representation of steel suffers from the following drawbacks:

1. In the case of curved or complicated bar geometry a distorted shell element needs to be used to match the bar geometry.
2. The bar must be assumed to lie in the mid-surface of the shell element, as shown in Fig.2, where the nodes of the parent element are located. So the finite element mesh patterns are restricted by the location of reinforcement and consequently by the increase in the number of concrete elements and total degrees of freedom.

In order to achieve the advantages of a regular mesh, and at the same time model complicated reinforcing details, an embedded representation of reinforcement appears to be the desirable approach. Even so, the present embedded reinforcement models, when applied to problems with curved or draped reinforcement the prestressing tendons impose significant constraints on the selection of the overall mesh. A need therefore exists, for curved embedded representation of reinforcement that allows the choice of mesh to be somewhat independent of the reinforcement geometry and location.

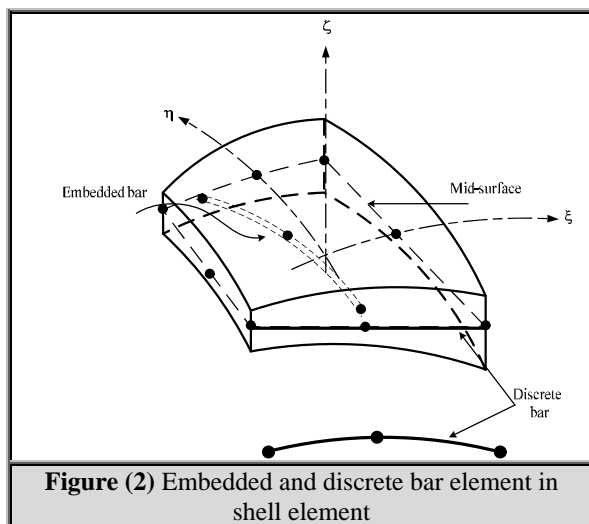


Figure (2) Embedded and discrete bar element in shell element

Phillips and Zienkiewicz [3], introduced the embedded representation of reinforcement. In their derivation, the reinforcing bar is restricted to lie

along the local coordinates, ξ or η of the parent element. Ranjbaran [4], modified the representation adopted above to account for inclined bars, using one-dimensional bar element with two nodes embedded in 8-node two-dimensional concrete element. The current formulation is based on modifying the above representation by using three-node one-dimensional bar element embedded inside the degenerated concrete shell element shown in Fig.3, which can represent inclined and/or curved tendons, using two Gaussian points.

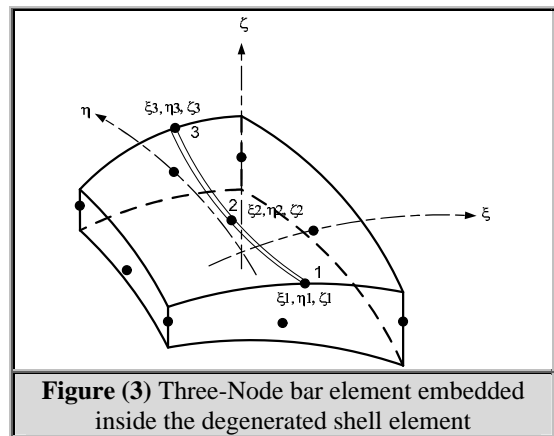


Figure (3) Three-Node bar element embedded inside the degenerated shell element

3. Prestressing Force Modeling

There are different methods to represent prestressing. The simplest one is that used by Lin and applied by Abdulla [5] and by Roca and Mari [6]. In this method the tendon is assumed to be frictionless and may be replaced by two types of in-plane forces, two end anchorage forces and a uniform pressure along the span of the member. The uniform pressure along the tendon may be replaced by a uniform distributed in-plane load along a line parallel to the longitudinal axis of the member.

Another method is that used by Ghalib[7], in which very sophisticated prestressing tendon models were used for modeling the interaction between the concrete and the housed tendon. In this method, prestressing tendons were considered as an integral part of the structure and a generally curved tendon element embedded in an isotropic flat shell element was developed.

In the present study a method similar to that used by Jirousek and Bouberguig [8], in which the equivalent load method is used to compute the force applied by the tendon on the structure, in the long direction only of the post-tensioned curved box-girder.

Using the global Cartesian coordinates of the tendon's nodal points (cb1, cb2, cb3), the Cartesian

coordinates of any other point on the tendon element can be obtained as follows:

$$cb = \sum_{i=1}^3 M_i(\tau) cb_i \Rightarrow$$

$\left. \begin{aligned} cb_x &= M_1 cb_{1x} + M_2 cb_{2x} + M_3 cb_{3x} \\ cb_y &= M_1 cb_{1y} + M_2 cb_{2y} + M_3 cb_{3y} \\ cb_z &= M_1 cb_{1z} + M_2 cb_{2z} + M_3 cb_{3z} \end{aligned} \right\} \quad \mathbf{1}$
--

where cb_{1x} , cb_{1y} , and cb_{1z} , are the global Cartesian coordinates of the tendon nodal point cb_1 , shown in Fig.4, and M_1 , M_2 , and M_3 are:

$M_1 = \frac{1}{2} \tau (\tau - 1)$	2
-------------------------------------	----------

$M_2 = (1 - \tau)^2$	3
----------------------	----------

$M_3 = \frac{1}{2} \tau (\tau + 1)$	4
-------------------------------------	----------

Also the variation of the tension force in the tendon will be defined in a form consistent with the definition of the tendon geometry, namely:

$T = \sum_{i=1}^3 M_i(\tau) T_i$	5
----------------------------------	----------

where T_i ($i = 1, 2, 3$) are given magnitudes of the tension at the nodal points.

To represent the effect of the prestressing in any tendon analytically by means of the equivalent load concept, the tendon has to be replaced by a set of three forces corresponding to the actual load imposed by the tendon.

A representation of a differential segment of a prestressing tendon is shown in Fig.5. The action of a prestressing tendon on a particular element may be represented by a distributed line load acting on the element along the corresponding segment of the tendon axis.

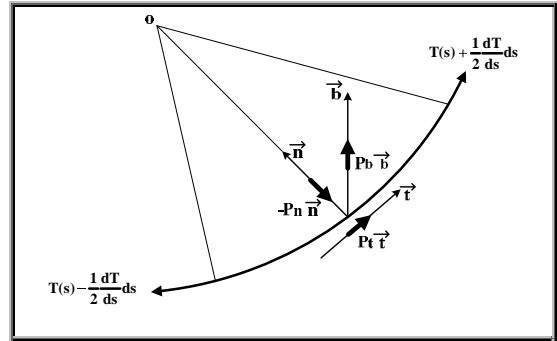


Figure (5) Equilibrium of a space tendon segment [6]

Due to the null bending stiffness, only an axial force can exist at any point of the tendon.

The equilibrium condition can be written as:

$\begin{aligned} -\left(T(s) - \frac{1}{2} \frac{dT}{ds} ds\right) \left(\vec{t} - \frac{1}{2} \frac{d\vec{t}}{ds} ds\right) + \left(T(s) + \frac{1}{2} \frac{dT}{ds} ds\right) \left(\vec{t} + \frac{1}{2} \frac{d\vec{t}}{ds} ds\right) \\ + (P_t \vec{t} + P_n \vec{n} + P_b \vec{b}) ds = 0 \end{aligned}$	6
--	----------

Operating and neglecting the second order terms yields:

$T \frac{d\vec{t}}{ds} + \frac{dT}{ds} \vec{t} = -P_t \vec{t} - P_n \vec{n} - P_b \vec{b}$	7
--	----------

Using the following geometric relationship:

$\frac{d\vec{t}}{ds} = \frac{\vec{n}}{R}$	8
---	----------

where R is the radius of the principal curvature, giving:

$T \frac{\vec{n}}{R} + \frac{dT}{ds} \vec{t} = -P_t \vec{t} - P_n \vec{n} - P_b \vec{b}$	9
--	----------

or, in a scalar form:

$P_n = -\frac{T}{R}$	10
----------------------	-----------

$P_t = -\frac{dT}{ds}$	11
------------------------	-----------

$P_b = 0$	12
-----------	-----------

The global Cartesian components of the unit vectors \vec{t} and \vec{n} may be written as:

$$\vec{t} = \frac{\vec{v}_t}{|\vec{v}_t|} \quad \text{with} \quad \vec{v}_t = \frac{dcb}{d\tau} \quad 13$$

$$\vec{v}_t = \sum_{i=1}^3 \frac{dM_i(\tau)}{d\tau} cb_i \quad 14$$

$$\left. \begin{aligned} v_{tx} &= \frac{dM_1}{d\tau} cb_{1x} + \frac{dM_2}{d\tau} cb_{2x} + \frac{dM_3}{d\tau} cb_{3x} \\ \Rightarrow v_{ty} &= \frac{dM_1}{d\tau} cb_{1y} + \frac{dM_2}{d\tau} cb_{2y} + \frac{dM_3}{d\tau} cb_{3y} \\ v_{tz} &= \frac{dM_1}{d\tau} cb_{1z} + \frac{dM_2}{d\tau} cb_{2z} + \frac{dM_3}{d\tau} cb_{3z} \end{aligned} \right\} \quad 15$$

$$|\vec{v}_t| = \sqrt{(v_{tx})^2 + (v_{ty})^2 + (v_{tz})^2} \quad 16$$

$$\therefore \begin{Bmatrix} \vec{t}_x \\ \vec{t}_y \\ \vec{t}_z \end{Bmatrix} = \frac{1}{|\vec{v}_t|} \begin{Bmatrix} v_{tx} \\ v_{ty} \\ v_{tz} \end{Bmatrix} \quad 17$$

and, $\vec{n} = \frac{\vec{v}_n}{|\vec{v}_n|}$ with

$$\vec{v}_n = \frac{1}{|\vec{v}_t|^2} \left(\frac{d^2cb}{d\tau^2} - \frac{a_t}{|\vec{v}_t|^2} \frac{dcb}{d\tau} \right) \quad 18$$

$$a_t = \frac{d^2cb}{d\tau^2} \frac{dcb}{d\tau} \quad 19$$

The combination of the global components of the tangential normal loads can be defined as:

$$\mathbf{P} = \begin{Bmatrix} P_x \\ P_y \\ P_z \end{Bmatrix} = P_t \vec{t} + P_n \vec{n} \quad 20$$

where,

$$P_t = -\frac{dT}{ds} = -\frac{1}{|\vec{v}_t|} \frac{dT}{d\tau} \quad 21$$

$$P_n = -\frac{T}{R} = -|\vec{v}_n| T \quad 22$$

When one of the end points of the tendon element (cb1 or cb3) coincides with the end of the tendon, shown in Fig.6, the end anchoring force ($P_1 = T_1$) or ($P_m = -T_m$) must be applied to the element as a concentrated local load. This load, tangential to the tendon axis, will most conveniently be specified by giving the vector of its Cartesian global components:

$$P_1 = \begin{Bmatrix} P_{x1} \\ P_{y1} \\ P_{z1} \end{Bmatrix} = (T \cdot \vec{t})_{\tau=-1} \quad 23$$

$$P_m = \begin{Bmatrix} P_{xm} \\ P_{ym} \\ P_{zm} \end{Bmatrix} = -(T \cdot \vec{t})_{\tau=+1} \quad 24$$

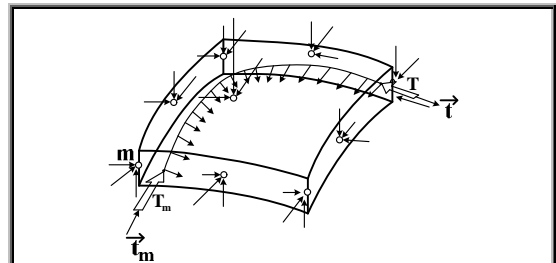


Figure (6) Work equivalent node forces caused by prestressing on a concrete finite element [6]

Using the following Eq. to define the displacement of the element:

$$\{u\} = [N] \{\delta\} \quad 25$$

and assuming that the element is traversed by only one prestressing tendon. Then, using the principle of virtual work to show that the local loads given through Eq.s (13) to (22) are balanced by the primary nodal forces FPr of the element leads to:

$$F_{Pr} = - \int_{\ell} N^T(\xi_{cb}, \eta_{cb}, \zeta_{cb}) P(\tau) ds - \left[\begin{array}{l} N^T(\xi_{cb1}, \eta_{cb1}, \zeta_{cb1}) P_1 \text{ or} \\ N^T(\xi_{cbm}, \eta_{cbm}, \zeta_{cbm}) P_m \end{array} \right] \quad 26$$

$$F_{Pr} = - \int_{-1}^{+1} N^T(\xi_{cb}, \eta_{cb}, \zeta_{cb}) P(\tau) |v_t(\tau)| d\tau - \left[\begin{array}{l} N^T(\xi_{cb1}, \eta_{cb1}, \zeta_{cb1}) P_1 \text{ or} \\ N^T(\xi_{cbm}, \eta_{cbm}, \zeta_{cbm}) P_m \end{array} \right] \quad 27$$

The large brackets, containing the end anchoring forces, have been used to indicate that the use of these terms is limited to cases where the point cb1 or cbm coincides with the end of the tendon. If more than one tendon traverses the element considered, the effect of each one is computed separately, using Eq. (27) and the results are summed.

4. Applications and Results

A computer program has been developed to carry out the nonlinear finite element analysis of prestressed concrete members under the effect of static loading.

The program developed and used in this study is based, on the computer programs PLAST by Huang [9], PLSHELL and CONCR1 by Hinton and Owen [10].

The new computer program includes all material nonlinearities, prestressing tendons are modeled by a multi-linear five branch stress-strain relationship.

A numerical example is analyzed using the developed computer program, to test the program capabilities and to show the applicability and the accuracy of the proposed method for tendons representation and inclusion of the effect of prestressing force in prestressed concrete members. The analyzed slab is chosen from three simply supported prestressed concrete slabs tested experimentally by Perry and Okafor [11], which is designated as A8. The slab is square with plan dimensions of 1.5x1.5 m and a uniform thickness of 60 mm, resting on simple edge supports, and has its corners held down, as shown in Fig.7. The prestressing was applied in both directions by straight bonded 7-mm diameter wires. The distribution of elements and tendons profile is shown in Fig.8. For numerical purposes, the loading is applied centrally through a 152 mm diameter flat steel platen, this circular platen is transformed to an equivalent square platen having a side length of 135

mm. Due to symmetry, only one quarter of the slab is considered in the finite element analysis.

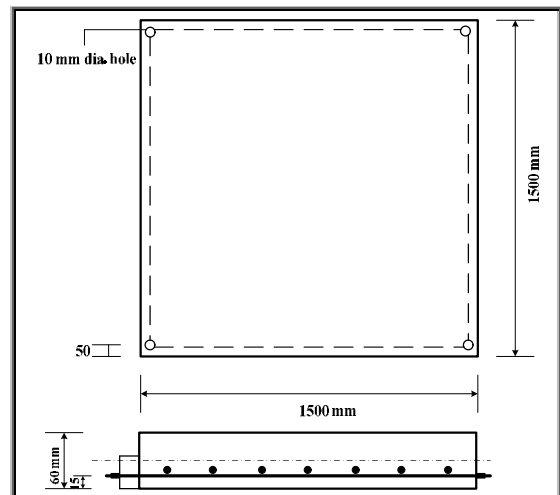


Figure (V) Details of prestressed concrete slab tested by Perry and Okafor[11]

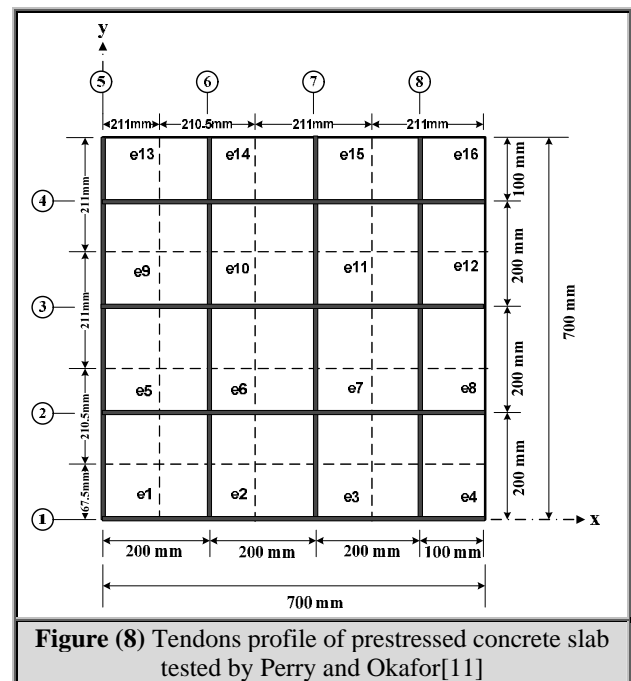


Figure (8) Tendons profile of prestressed concrete slab tested by Perry and Okafor[11]

The material properties of concrete are: Young's modulus, $E_c = 35100$ MPa, compressive strength, $f'_c = 57$ MPa, tensile strength, $f'_t = 3.84$ MPa, Poisson's ratio, $\nu = 0.18$, and ultimate compressive strain, $\epsilon_{cu} = 0.0035$.

The material properties of prestressing tendons are: yield stress = 1289 MPa, ultimate stress = 1931 MPa, area of a prestressing tendon = 38.5 mm²,

effective prestressing stress = 1128 MPa, curvature friction coefficient = 0.15 rad-1, and wobble friction coefficient = 0.001 m-1.

Comparison between the numerical and the experimental results of the load-deflection curves is shown in Fig.9, from which very good agreement is seen through all loading levels. The computed ultimate load value is 93 kN, whereas the ultimate load value obtained experimentally [11] is 97 kN. The ratio of the ultimate computed load to the experimental value is 0.959.

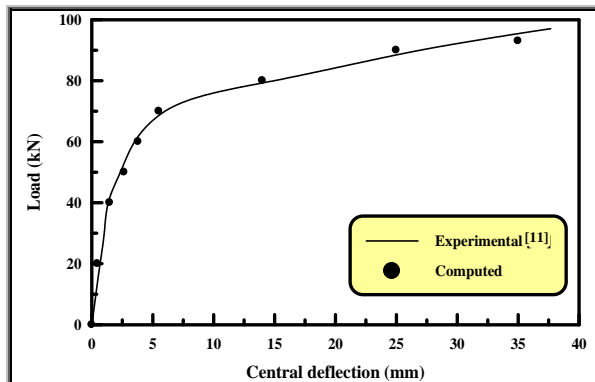


Figure (9) Comparison between computed and experimental load-deflection curves

Fig.10, shows the variation of the average longitudinal stress along different tendons with the applied load. The curves represent the longitudinal stresses in the part of tendon 1 included in element 1, and the part of tendon 2 included in element 5. It is noticed that, the longitudinal stress in tendon 1 increases significantly after cracks appearance at about 32% of the ultimate load.

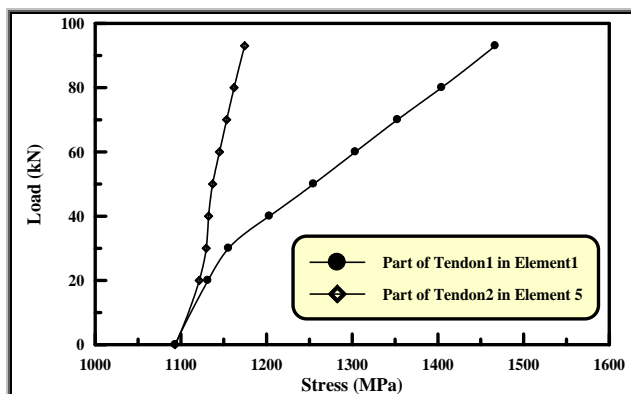


Figure (10) Variation of longitudinal stress in tendons with applied load

The variation of the longitudinal stresses in tendons 1 and 8 at ultimate load with the distance from the central point of the slab is shown in Fig.11. It is seen that, the longitudinal stress in tendon 1

decreases with the increase of distance from the center of slab (loading position), whereas the longitudinal stress in tendon 8 seems to have a little increase with the distance.

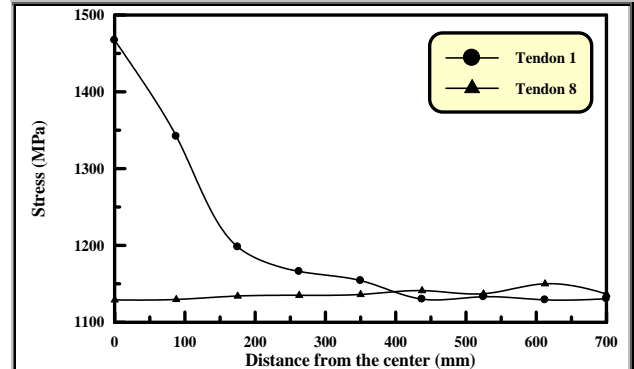


Figure (11) Variation of longitudinal stresses with distance in tendons at ultimate load

5. Conclusion

The 8-noded degenerated shell element and the constitutive relations and the method used in this investigation have been successfully used utilizing the developed computer program to predict the behavior and load carrying capacity of prestressed concrete members. The used development for modeling prestressing tendons as embedded bars within the parent concrete element gave very good results in comparison with the experimental results.

6. Notations

cb1, cb2, cb3:	Tendon's nodal points
cb _{1x} , cb _{1y} , cb _{1z} :	Global Cartesian coordinates of nodal point cb ₁
E _c :	Modulus of elasticity of concrete
F _{Pr} :	Element's primary nodal force caused by prestressing
f' _C :	Ultimate compressive strength of concrete
f' _t :	Uniaxial tensile strength of concrete
M1, M2, M3:	Shape functions of the embedded bar
N:	Shape function of element nodes
P _x , P _y , P _z :	Global components of prestressing force
T _i :	Tension force at tendon nodal

	point i
u :	Displacement in global x -direction
τ :	Dimensionless coordinate along the embedded bar element
ξ, ζ, η :	Natural coordinate system

7. References

- [1] Chan E. C., "Nonlinear Geometric, Material and Time-Dependent Analysis of Reinforced Concrete Shells with Edge Beams," Ph. D. Dissertation, University of California, Berkeley, USA, 1983.
- [2] Ahmad, S., Irons, B. M., and Zienkiewicz, O. C., "Analysis of Thick and Thin Shell Structures by Curved Finite Element," *Int. J. for Numerical Methods in Engineering*, Vol. 2, No. 3, pp. 419-451, Jul.-Sept. 1970.
- [3] Phillips, D. V., and Zienkiewicz, O. C., "Finite Element Nonlinear Analysis of Concrete Structures," *Proc. Inst. of Civil Engineers, Part 2*, Vol. 61, pp. 59-88, 1976.
- [4] Ranjbaran, A., "Embedding of Reinforcements in Reinforced Concrete Elements Implemented in DENA," *Computers and Structures*, Vol. 40, No. 4, pp. 925-930, 1991.
- [5] Abdulla, M. A., and Abdul-Razzak A. A., "Finite Strip Analysis of Prestressed Box-Girder," *Computers and Structures*, Vol. 36, No. 5, pp. 817-822, 1990.
- [6] Roca, P., and Mari, A. R., "Numerical Treatment of Prestressing Tendons in The Nonlinear Analysis of Prestressed Concrete Structures," *J. of Computers and Structures*, Vol. 46, No. 5, pp. 905-916, May 1993.
- [7] Ghalib, A. M., "Inelastic Finite Element Analysis of Prestressed Concrete Multi-Planar System," M.Sc. Thesis, University of Baghdad, 1990.
- [8] Jirousek, J., and Bouberguig A., "A Macro-Element Analysis of Prestressed Curved Box-Girder Bridges," *J. of Computers and Structures*, Vol. 10, No. 3, pp. 467-482, June 1979.
- [9] Huang, H. C., "Static and Dynamic Analyses of Plates and Shells," Springer-Verlag U. K., 1st ed., 1989.
- [10] Hinton, E., and Owen, D. R. J., "Finite Element Software for Plates and Shells," Pineridge Press U. K., 1st ed., 1984.
- [11] Perry, S. H., and Okafor, H. O., "Collapse of Square Prestressed Concrete Slabs with Corner Restraint," *J. of Structural Engineering, ASCE*, Vol. 111, No. 2, pp. 307-327, Feb. 1985.

التحليل اللاخطي للأعضاء الخرسانية مسبقة الجهد بطريقة العناصر المحددة

د. زبيدة عبداللطيف البياتي

مدرس

قسم الهندسة المدنية / الجامعة المستنصرية

د. هاني محمد فهمي

استاذ

قسم الهندسة المدنية / جامعة النهرين

الخلاصة

استخدمت طريقة العناصر المحددة لتحليل مقاومة و تصرف الاعضاء الخرسانية المسبقة الجهد تحت تأثير الأحمال القصيرة و الطويلة الأمد، حيث تم استخدام العنصر القشري المولد و المؤلف من ثمانية عقد و لكل عقدة خمسة درجات حرية للحركة. كذلك تم اعتماد الخصائص اللاخطية للمادة، حيث تم اعتبار الخرسانة مادة خطية مرنة-لدنة لها صلادة الإنفعال (strain hardening) تحت تأثير الإنضغاط. بينما تم تمثيل علاقة الإجهاد- الإنفعال للقضبان المسبقة الإجهاد بعلاقة خطية متعددة الاجزاء مؤلفة من خمسة أجزاء. استخدمت طريقة الطبقات (layered approach) في تمثيل الخرسانة، أما القضبان المسبقة الجهد فقد تم تمثيلها كأعضاء أحادية المحور مطمورة في العنصر الخرساني. تم تطوير وإستخدام برنامج حاسوب لإجراء التحليلات للأعضاء الخرسانية المسبقة الجهد التي لها شكل مختلف لتوزيع القضبان المسبقة الجهد في حالتي الشد المسبق و الشد اللاحق. يحدد شكل قضبان تسبيق الجهد و يقوم البرنامج بحساب الحمل الناتج عن تسبيق الجهد. تم إثبات صحة الطريقة و العلاقات المقترحة لتمثيل القضبان المسبقة الإجهاد كأعضاء مطمورة، و آلية تمثيل القوى الناتجة من تسليط الإجهاد في القضبان المسبقة الجهد و توزيعها على العضو الخرساني المسبق الجهد. كما تم التأكد من صلاحية البرنامج المعد بتحليل عدد من الامثلة التي قد تم فحصها مختبرياً سابقاً. تمت مقارنة نتائج التحليلات مع النتائج العملية و قد كانت النتائج التحليلية جيدة مما يؤكد صحة و ملائمة الطريقة و صحة النماذج المقترحة و المستخدمة في الحل.

This document was created with Win2PDF available at <http://www.daneprairie.com>.
The unregistered version of Win2PDF is for evaluation or non-commercial use only.